Synthesis, Magnetic Characterization, and Sensing Applications of Novel Dextran-Coated Iron Oxide Nanorods

Sudip Nath,[†] Charalambos Kaittanis,[†,‡] Vasanth Ramachandran,[§] Naresh S. Dalal,[§] and J. Manuel Perez*,[†,‡,ǁ]

Nanoscience Technology Center, Burnett School of Biomedical Sciences, College of Medicine, and Department of Chemistry, University of Central Florida, Orlando, Florida 32826, and Department of Chemistry and Biochemistry, Florida State University, Tallahassee, Fl 32306

Monodisperse, water-soluble dextran-coated iron oxide (Fe_3O_4) nanorods were synthesized using a facile and scalable approach. Our room temperature method involves the mixing of an acidic solution of iron salts with a basic solution of ammonium hydroxide to facilitate initial formation of iron oxide crystals. The stability, crystallinity, and shape of these nanorods depends on the time of addition of the dextran, as well as the degree of purity of the polymer. The as-synthesized nanorods exhibit unique magnetic properties, including superparamagnetic behavior and high spin−spin water relaxivity (R2). Additionally, they possess enhanced peroxidase-like activity when compared to those reported in the literature for spherical iron oxide nanoparticles. Thus, this high yield synthetic method for polymer-coated iron oxide nanorods will expedite their use in applications from magnetic sensors, devices, and nanocomposites with magnetic and catalytic properties.

Introduction

Iron oxide-based magnetic nanoparticles have been widely used in a variety of biomedical applications such as magnetic separation,[1] magnetic resonance imaging,[2] hyperthermia,[3,4] magnetically guided drug delivery,[5,6] tissue repair,[3] and molecular diagnostics.[7−9] For most applications, a polymeric coating is needed to improve the nanoparticles' aqueous stability, biocompatibility, and conjugation properties. For instance, dextran-coated iron oxide nanoparticles have been successfully used as magnetic resonance imaging (MRI) contrast agents because of their strong ability to dephase water protons in surrounding tissue, which results in a decrease in the MRI signal.[10] In addition, the dextran coating can be cross-linked and functionalized with amino groups to facilitate the conjugation of targeting ligands for MRI and in vitro diagnostics applications.[11] Current synthetic procedures for dextran-coated iron oxide nanoparticles involve the formation of the iron oxide core in the presence of dextran, as stabilizer and capping agent.[12] Under these in situ conditions, the nature, quality, and amount of the polymer modulate the nucleation, growth, and size of the newly formed iron oxide nanocrystal. A common characteristic of most reported in situ dextran-coated iron oxide nanoparticles synthetic procedures is the formation of nanoparticles with a spherical iron oxide core.

Research efforts have been geared toward the production of small, uniform and highly dispersed spherical nanocrystals. Only recently, the importance of the nanoparticles' shape has been recognized, in particular one-dimensional (1D) structures such as nanorods and nanotubes, because they exhibit unique properties that are different from their corresponding zero dimensional counterparts (0D or spherical nanocrystals). Particularly in the case of iron oxide, 1D nanorods have been found to exhibit interesting magnetic properties because of their shape anisotropy, such as higher blocking temperatures and larger magnetization coercivity, compared to their 0D counterparts.[13−16] However, their wide application in biomedical research has been hampered by difficult procedures, use of toxic reagents,[17] and poor yields. For instance, current methods for iron oxide

* Corresponding author. E-mail: jmperez@mail.ucf.edu

† Nanoscience Technology Center, University of Central Florida.
‡ College of Medicine, University of Central Florida.
§ Florida State University.
ǁ Department of Chemistry, University of Central Florida.

(1) Wang, D. H., J.; Rosenzweig, N.; Rosenzweig, Z. *Nano Lett.* **2004**, *4*, 409–413.
(2) Baghi, M.; Mack, M. G.; Hambek, M.; Rieger, J.; Vogl, T.; Gstoettner, W.; Knecht, R. *Anticancer Res.* **2005**, *25* (5), 3665–70.
(3) Gupta, A. K.; Gupta, M. *Biomaterials* **2005**, *26* (18), 3995–4021.
(4) Ito, A.; Kuga, Y.; Honda, H.; Kikkawa, H.; Horiuchi, A.; Watanabe, Y.; Kobayashi, T. *Cancer Lett.* **2004**, *212* (2), 167–75.
(5) Kohler, N.; Sun, C.; Wang, J.; Zhang, M. *Langmuir* **2005**, *21* (19), 8858–64.
(6) Gupta, A. K.; Curtis, A. S. *J. Mater. Sci. Mater. Med.* **2004**, *15* (4), 493–6.
(7) Perez, J. M.; Josephson, L.; O'Loughlin, T.; Hogemann, D.; Weissleder, R. *Nat. Biotechnol.* **2002**, *20* (8), 816–20.
(8) Perez, J. M.; O'Loughin, T.; Simeone, F. J.; Weissleder, R.; Josephson, L. *J. Am. Chem. Soc.* **2002**, *124* (12), 2856–7.
(9) Perez, J. M.; Simeone, F. J.; Saeki, Y.; Josephson, L.; Weissleder, R. *J. Am. Chem. Soc.* **2003**, *125* (34), 10192–3.
(10) Perez, J. M.; Josephson, L.; Weissleder, R. *Chembiochem* **2004**, *5* (3), 261–4.
(11) Josephson, L.; Tung, C. H.; Moore, A.; Weissleder, R. *Bioconjugate Chem.* **1999**, *10* (2), 186–91.
(12) Thorek, D. L.; Chen, A. K.; Czupryna, J.; Tsourkas, A. *Ann. Biomed. Eng.* **2006**, *34* (1), 23–38.
(13) Peng, X.; Manna, L.; Yang, W.; Wickham, J.; Scher, E.; Kadavanich, A.; Alivisatos, A. P. *Nature* **2000**, *404* (6773), 59–61.
(14) Hu, J.; Li, L.; Yang, W.; Manna, L.; Wang, L.; Alivisatos, A. P. *Science* **2001**, *292* (5524), 2060–3.
(15) Puntes, V. F.; Krishnan, K. M.; Alivisatos, A. P. *Science* **2001**, *291* (5511), 2115–7.
(16) Melosh, N. A.; Boukai, A.; Diana, F.; Gerardot, B.; Badolato, A.; Petroff, P. M.; Heath, J. R. *Science* **2003**, *300* (5616), 112–5.

nanorods involve hydrothermal,[18,19] sol−gel,[20] and high-temperature procedures,[17,21] among others. Therefore, water-based synthetic procedures for iron oxide nanorods that are simple, economical, low temperature, and high yield are in high demand. In particular, synthetic methods that yield water-soluble and stable polymer-coated nanorods would be ideal for studies geared toward the development of magnetic biosensors and magnetic devices.

Here we report a facile, high-yield, room-temperature, and water-based synthetic protocol that yields disperse dextran-coated iron oxide nanorods (DIONrods). Our synthetic procedure differs from those previously reported methods for dextran-coated iron oxide nanoparticles in that the dextran is not present during the initial nucleation process. Instead, the dextran is added at a later stage. This "stepwise" process, as opposed to the in situ process, allows the formation of stable, disperse, and highly crystalline iron oxide nanorods that exhibit supermagnetic behavior and improved high water relaxivity. First, we used these nanorods as magnetic nanosensors for the sensitive and fast detection of a particular bacterium in milk, achieving a detection limit of 6 cfu (colony forming units) in just 5 min. Next, the peroxidase-like activity of the as-synthesized rods was also evaluated, demonstrating that our DIONrods possess enhanced peroxidase activity as compared to their spherical counterparts. Finally, studies using dextrans with various degrees of purity revealed that rod formation is favored when a highly pure polymer is used.

Materials and Methods

Materials. Iron salts, $FeCl_2 \cdot 4H_2O$, and $FeCl_3 \cdot 6H_2O$ were purchased from Sigma. Dextran (10 kDa) was received from Amersham Biosciences and Sigma. Sulfo-*N*-hydroxysuccinimide-LC-Biotin, disuccinimidyl suberate (DSS) and *N*-Succinimidyl 3-(2-pyridyldithio)-propionate (SPDP) were purchased from Pierce. The peroxidase-sensitive dye 3,3′,5,5′-tetramethylbenzidine (TMB), protein G, and concanavalin A were received from Sigma. The anti-MAP antibody and MAP bacteria were kindly supplied by Dr Saleh Naser from the Microbiology and Molecular Biology Department, University of Central Florida.

Synthesis of Iron Oxide Nanoparticles. An acidic solution of iron salts containing 0.203 g of $FeCl_2 \cdot 4H_2O$ and 0.488 g of $FeCl_3 \cdot 6H_2O$ in HCl solution (88.7 μL of 12 N HCl in 2 mL of water) was mixed with ammonium hydroxide solution (830 μL of NH_4OH in 15 mL of DI water) under stirring conditions using a digital vortex meter. The reaction mixture turned black instantaneously and after a few seconds (θ) of stirring, a solution of dextran (5 g in 10 mL of DI water) was added to yield dextran-coated iron oxide nanoparticles. The resultant solution continued to be stirred for 1 h and was then centrifuged at 13 000 rpm for 30 min to get rid of large particles. The supernatant was collected, washed several times with distilled water, and concentrated through an Amicon 8200 cell (Millipore ultrafiltration membrane YM − 30 k). This results in dextran-coated iron oxide nanorods (DIONrods). To prepare aminated nanoparticles, 3 mg (i.e.,

3 mL of solution containing ∼1 mg of iron/mL) of DIONrod suspension in water was treated with 5 mL of 0.5 M NaOH and 200 μL of epicholohydrin. The mixture was stirred vigorously at room temperature for 8 h. Afterward, 850 μL of 30% ammonia was added and stirred for 12 h to complete the amination procedure. The free epichlorohydrin was removed by washing the solution repeatedly with distilled water using Amicon cell. The resulting aminated DIONrods are highly stable in water and phosphate buffer saline for months.

Characterization. The particles were characterized using HR-TEM (FEI TECNAI F30), XPS (Physical Electronics 5400 ESCA) and XRD (Rigaku D/MAX XRD) techniques. T2 was measured using a Bruker Minispec mq20 NMR analyzer operating at 0.47 T at 37 °C. A Quantum Design SQUID magnetic property measurement system (MPMS XL) was used to perform all the magnetic measurements on the Fe_3O_4 nanoparticles. Zero-field-cooled (ZFC) and field-cooled (FC) measurements of dc magnetic susceptibility were done using a 200 G field, by varying the temperature from 1.8 to 250 K. In the ZFC process, the sample was first cooled under zero external magnetic field, followed by the application of $H =$ 200 G, whereas in the FC process, the sample was cooled in the presence of magnetic field $H =$ 200 G, before sweeping the temperature. Hysteresis loops were measured at temperatures 5, 100, and 200 K with the magnetic field varying from −2 to 2 T. Zero field ac magnetic susceptibility as a function of temperature was measured at frequencies ranging from 0.01 Hz to 1 kHz, using a drive field of 5 G. The amount of iron present per ml of solution was determined using acid digestion method. The quantification of amines present on the surface of the aminated DIONrods was done as described.[11]

Synthesis of MAP Nanosensors and Detection of MAP Bacteria in Milk. The aminated DIONrods were centrifuged at 13 000 rpm and the pellet was redispersed in DMSO. The nanorods suspension in DMSO (650 μL, 0.1 mg Fe/mL) was then incubated with 6.89 mg of disuccinimidyl suberate (DSS) for 12 h at room temperature. The reaction mixture was then centrifuged and the pellet was washed and redispersed in PBS. Finally, the modified nanorods were incubated with protein G (1 mg/ml) and kept for 12 h at 4 °C. The excess protein G was removed by magnetic separation using a MACS magnetic column and the amount of protein G was assessed by protein assay as described.[9,22]

The resulting protein G-conjugated nanorods (protein G DION-rods) were treated with anti-MAP-antibody (10 μL) and incubated overnight in order to facilitate a stable protein G−anti-MAP-antibody association. The average number of antibodies conjugated per nanoparticle was assessed as previously described.[9,11,22] The resulting anti-MAP DIONrods (200 μL) were used as magnetic nanosensors to detect MAP bacteria in milk (20 μL) and the changes in T2 were monitored using a 0.47T magnetic relaxometer (MiniSpec, Bruker) to detect the bacteria present in the sample.

Kinetic Assay of DIONrods Peroxidase Activity. The peroxidase activity of the iron oxide nanoparticles was evaluated via steady-state kinetic assays at room temperature. Specifically, serial dilutions of TMB were prepared in citrate buffer (pH 4), and 100 μL aliquots were dispensed in a 96-well plate. Subsequently, aliquots of either the corresponding DIONrod preparations, having equal iron concentrations (2 μg per mL), were added to the wells. After addition of 25 μL of H_2O_2 (30%), each well's absorbance was recorded at 652 nm, using a Synergy HT microtiter plate reader (Biotek).The kinetic parameters were determined via the Michaelis−Menten equation: $\iota = V_{max} [S]/(K_m + [S])$, where ι is the initial rate of reaction, V_{max} is the maximum rate of reaction, [S] is the substrate's concentration, and K_m is the Michaelis constant.

(17) Park, S. J.; Kim, S.; Lee, S.; Khim, Z. G.; Char, K.; Hyeon, T. *J. Am. Chem. Soc.* **2000**, *122* (35), 8581–8582.

(18) Wang, J. P., Z. M.; Huang, Y. J.; Chen, C. W. *J. Cryst. Growth* **2004**, *263*, 616–619.

(19) Zhao, Y. M.; Li, Y. H.; Ma, R. Z.; Roe, M. J.; McCartney, D. G.; Zhu, Y. Q. *Small* **2006**, *2* (3), 422–427.

(20) Corr, S. A.; Gun'ko, Y. K.; Douvalis, A. P.; Venkatesan, M.; Gunning, R. D.; Nellist, P. D. *J. Phys. Chem. C* **2008**, *112* (4), 1008–1018.

(21) Wen, X.; Wang, S.; Ding, Y.; Wang, Z. L.; Yang, S. *J. Phys. Chem. B* **2005**, *109* (1), 215–20.

(22) Kaittanis, C.; Naser, S. A.; Perez, J. M. *Nano Lett.* **2007**, *7* (2), 380–3.

Table 1. Effect of the Time of Addition of Dextran (θ) on the R2 Relaxivity of the DIONrods

time of addition of dextran (θ)	R2 (mM^{-1} s^{-1})
before adding ammonia	<1
1 s	50 ± 2
10 s	150 ± 7
30 s	300 ± 5
60 s	300 ± 9

Results and Discussions

In our first set of experiments, we optimized the synthetic protocol, including the order of addition (in situ vs stepwise), and the time of addition of the dextran polymer. Our water-based synthetic protocol involves an acid−base reaction between an acidic solution of iron salts and a basic solution of ammonium hydroxide. Upon mixing, the resulting solution becomes alkaline (pH 9.0), facilitating the formation of iron oxide nanocrystals. This initial formation of nanocrystals can occur either in the presence (in situ) or absence (stepwise) of dextran. Because most synthetic procedures that afford stable and monodisperse nanoparticles use an in situ approach, we opted to follow this approach first. In these experiments, a mixture of iron salts ($FeCl_3 \cdot 6H_2O$ and $FeCl_2 \cdot 4H_2O$) was dissolved in an aqueous solution of HCl, whereas a dextran solution was prepared in aqueous ammonia solution and placed on a digital vortex meter. Next, the acidic iron salt solution was poured into the ammonia solution of dextran under vigorous stirring condition. Following this protocol, we obtained poorly crystalline, spherical nanocrystals of 20 ± 5 nm in diameter and poor R2 relaxivity (<1 mM^{-1} s^{-1}). This poor relaxivity contrasts with the relaxivity obtained with other published in situ procedures where relaxivity values between 60 and 100 mM^{-1} s^{-1} are obtained.

We then investigated if a stepwise approach will result in larger iron oxide nanocrystals and an improvement in R2 relaxivity. In this approach, a dextran solution was added at a particular time (θ) after initiating the iron oxide nanocrystal's nucleation process. In initial optimization experiments, we measured T2 relaxivity (R2) and obtained TEM images of a series of dextran coated iron oxide nanoparticles prepared after adding dextran at different (θ) times (1, 10, 30, and 60 s). Following this approach, we obtained nanorods for which their size and R2 relaxivity can be fine-tuned by varying the time of dextran's addition (θ) (Table 1). No significant difference was observed in the cystallinity and magnetic properties (particularly R2) of the nanorods synthesized at $\theta \geq 30$ s. However, the yield of the iron oxide nanorods was greatly reduced under these conditions ($\theta \geq 30$ s), based on measurements of the iron concentrations of the nanorods' suspension.[11,23] The observed low yield at $\theta \geq 30$ s could be due to the fact that a higher number of larger (micrometer-size) crystals are formed when the stabilizing agent (dextran) is added at a later time after initiation of the nucleation process. These micrometer-size particles tend to precipitate easily and are removed from suspension during the purification process. Because the most optimal preparation was obtained when dextran was added

30 s after initiating the iron oxide nucleation, we then adopted these conditions in our nanorods synthesis.

TEM studies (Figure 1a) of the DIONrods preparation (R2 = 300 mM^{-1} s^{-1}) reveal monodisperse rod-shaped iron oxide crystals, with an average length of 310 ± 10 nm and width of 135 ± 5 nm, for an aspect ratio of 2.3. Corresponding HRTEM (Figure 1b) analysis and selected area electron diffraction (**inset of** Figure 1b) confirm the formation of highly crystalline nanocrystals. X-ray diffraction pattern of DIONrods Figure 1c indicates eight distinct peaks at 18.2, 30.1, 35.6, 37, 44.2, 53.6, 57, and 62.5°, accounting for crystal planes 111, 200, 311, 222, 400, 422, 511, and 440. These X-ray diffraction data correspond to the formation of magnetite (Fe_3O_4) nanocrystals.[24] Meanwhile, XPS was performed to determine the oxidation state of the iron present. Two distinct peaks at 715 and 728 eV representing $Fe2p_{3/2}$ and $Fe2p_{1/2}$ orbital electrons, as shown in Figure 1d, confirmed the formation of magnetite in the solution.[25]

Using SQUID magnetometry, we studied the magnetic properties of the DIONrods.[26] First, hysteresis loops measured at three different temperatures (Figure 2a) demonstrated a coercivitiy of 500 ± 10 G at 5 K that disappeared at 100 and 200 K, which is typical of superparamagnetic behavior. Zero-field-cooled (ZFC) and field-cooled (FC) dc susceptibility studies (Figure 2b) show that the ZFC magnetic moment increased as the temperature increased, reaching a maximum at 28 K (the blocking temperature, T_B); it then decreased with a further increase in temperature. In the FC process, above the blocking temperature (T_B), the data followed the ZFC curve but deviated from ZFC curve below T_B, showing a slow increase in the moment with decreasing temperature. The maximum found in the ZFC curve (at T_B) is where a maximum number of particles exhibit superparamagnetic behavior. Below T_B, the relaxation times of the particles are longer than the experimental measurement time; hence the particles acquire a blocked state. In the ac susceptibility, both real and imaginary components $\chi'(T)$ and $\chi''(T)$, at different frequencies ranging from 1 Hz to 1kHz exhibited a frequency-dependent maximum (panels c and d in Figure 2), which shifted to higher temperatures with increasing frequency. This may be due to either spin glass or superparamagnetic behavior. To clearly distinguish between these two behaviors, we calculated the Mydosh parameter (Φ) from the real part of the ac susceptibility according to the following equation[27]

$$\Phi = \frac{\Delta T_m}{T_m[\Delta \log_{10}(\nu)]}$$

Here, T_M is the temperature corresponding to the observed maximum at the lower-frequency end.[27] We used the χ'(1

(23) Shen, T.; Weissleder, R.; Papisov, M.; Bogdanov, A., Jr.; Brady, T. J. *Magn. Reson. Med.* **1993**, *29* (5), 599–604.

(24) Jun, Y. W.; Huh, Y. M.; Choi, J. S.; Lee, J. H.; Song, H. T.; Kim, S.; Yoon, S.; Kim, K. S.; Shin, J. S.; Suh, J. S.; Cheon, J. *J. Am. Chem. Soc.* **2005**, *127* (16), 5732–3.

(25) Zou, G.; Xiong, K.; Jiang, C.; Li, H.; Li, T.; Du, J.; Qian, Y. *J. Phys. Chem. B* **2005**, *109* (39), 18356–60.

(26) Magana, D.; Perera, S. C.; Harter, A. G.; Dalal, N. S.; Strouse, G. F. *J. Am. Chem. Soc.* **2006**, *128* (9), 2931–9.

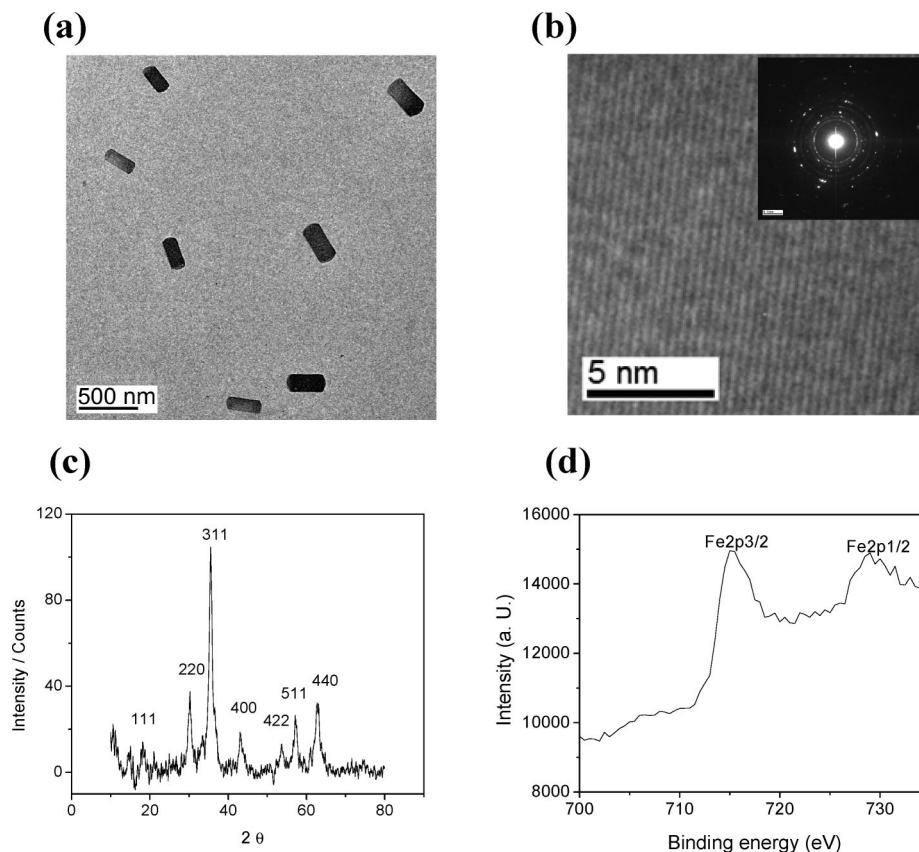(27) Mydosh, J. A. *Spin Glasses*; Taylor & Francis: Washington D.C., 1993.

(a)

(b)

(c)

(d)

Figure 1. (a) TEM, (b) HRTEM and SAED (inset), (c) XRD, and (d) XPS analyses of DIONrods.

Hz) and χ''(1kHz) data to calculate Φ. The calculated value of Φ is 0.072, which is close to the average value of $\sim$0.1 for superparamagnetic systems.[26−29] Taken together, these results show that our DIONrods exhibit superparamagnetic behavior.

Furthermore, we performed experiments to assess the quality and stability of our nanorods in aqueous suspensions. First, the presence of dextran on nanorods' surface was confirmed by performing clustering experiments with Con-canavalin-A (ConA).[30,31] Specifically, the presence of dextran on the nanoparticles' surface can be identified via ConA-induced nanoparticle clustering, due to the strong affinity and multivalency of ConA toward carbohydrates, such as dextran. DLS experiments (Figure 3a) show a time-dependent increase in particle size distribution upon ConA addition, due to formation of nanoparticle assemblies. Most importantly, a fast and reproducible change in T2 relaxation time was observed (Figure 3b), indicating not only the association of dextran with the nanoparticle but also the feasibility of our DIONrods as magnetic relaxation sensors.

FT-IR experiments (Figure 3c) further confirmed the presence of characteristic dextran peaks on the DIONrod preparations. Most importantly, the prepared DIONrods can

be concentrated in PBS by ultrafiltration, obtaining highly concentrated preparations without nanoparticle precipitation even upon storage at 4 °C for more than 12 months (see Figure 1 in the Supporting Information). Taken together, these results demonstrate the robustness of the dextran coating on the nanorods, making them suitable for biomedical applications.

These experiments encouraged us to study the use of our DIONrods as magnetic sensors for bacterial detection. The need for developing fast, sensitive, and reliable detection methods for bacteria in food, the environment, and clinical samples is crucial, in order to safeguard public health. We hypothesized that nanoparticles with larger R2 relaxivity would allow us to use lower amount of nanoparticles (lower amount of iron) and potentially improve the detection limit. We tested our hypothesis using *Mycobacterium avium* spp. *paratuberculosis* (MAP) as our model organism, because the identification of MAP using current methods is difficult due to the bacterium very slow growth. Recently, we reported the detection of MAP in milk with magnetic nanoparticles within 45 min.[22] Therefore, we examined if the iron oxide nanorods described herein, having enhanced magnetic properties, can improve the assay's bacterial detection kinetics. For these experiments, we first cross-linked and aminated the dextran of the iron oxide nanorods to yield aminated-DIONrods, before conjugation with anti-MAP antibodies via protein G as previously described.[22] The resulting anti-MAP DIONrods (2 μg of Fe per mL) were stable in aqueous solutions and complex media (e.g., PBS, milk) and had an average of 40 antibodies per nanoparticle. This high number

(28) Goya, G. F. B., T. S.; Fonseca, F. C.; M, P. *J. Appl. Phys.* **2003**, *94*, 3520.

(29) Culp, J. T.; Park, J. H.; Meisel, M. W.; Talham, D. R. *Inorg. Chem.* **2003**, *42* (9), 2842–8.

(30) Nath, S.; Kaittanis, C.; Tinkham, A.; Perez, J. M. *Anal. Chem.* **2008**, *80* (4), 1033–8.

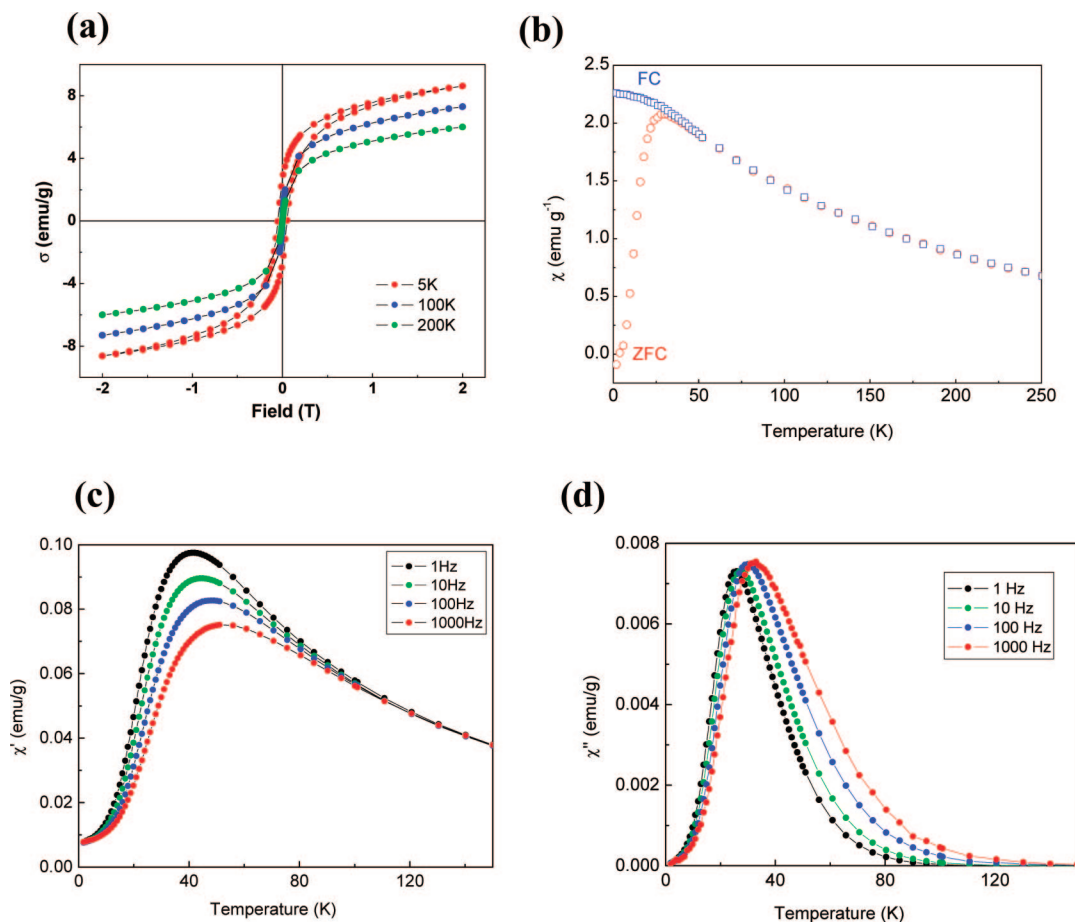(31) Perez, J. M.; Asati, A.; Nath, S.; Kaittanis, C. *Small* **2008**, *4* (5), 552–6.

(a)

(b)

(c)

(d)

Figure 2. (a) Hysteresis loops obtained at temperatures 5, 100, and 200 K; (b) zero-field-cooled (ZFC) and field-cooled (FC) magnetic susceptibilities in an external magnetic field $H = 200$ G; (c) real and (d) imaginary components of ac susceptibility at different frequencies.

of antibodies per particle is due to the larger volume (and therefore surface area) available for binding, which facilitates a larger number of protein G and antibody being conjugated per particle. In our first set of sensing experiments, we used the anti-MAP DIONrods to sense and quantify MAP bacteria in milk. Figure 4a shows a fast response of the anti-MAP DIONrods in the presence of bacteria (100 cfu or colony forming units) in milk, indicated by prominent changes in T2 that plateau at approximately 20 ± 1 ms, 30 min post-bacterial addition. In control experiments, using protein G conjugated DIONrods and no anti-MAP antibodies as well as in saturation experiments where the MAP bacteria was preincubated with the anti-MAP antibodies before sensing, no significant time-dependent increase in T2 was observed. These results to indicate that the fast and sensitive detection of MAP is dependent on the anti-MAP antibody attached to the nanorods.

These results encouraged us to perform dose-dependent experiments using lower bacterial concentrations and a shorter incubation time. We hypothesized that detection could be obtained within minutes after addition of the DIONrods, due to the nanorods' high R2 and the high number of antibodies per nanorods. For these experiments, bacterial solutions of MAP were prepared through serial dilutions in milk from an initial stock of 100 cfu of MAP. Afterward, a solution containing the DIONrods (2 μg of Fe per mL) was treated with 20 μL of the corresponding bacterial dilution and incubated for only 5 min at room temperature before

measurements were taken. The changes in the T2 relaxation times were monitored with respect to control containing same amount of nanosensor and 20 μL of milk. Results show a linear correlation between ΔT2 and the amount of MAP bacteria in cfu within 5 min of incubation (Figure 4b). Notably, the detection limit (6 cfu) and detection kinetics (5 min) of the assay in milk were improved when the nanorods were used as compared to previous reports with spherical nanoparticles.[22] Hence, the observed improvement in bacterial detection using the developed anti-MAP DIONrods can be attributed to both their high magnetic water relaxivity and their large number of antibodies per nanoparticle.

One of the most interesting properties of nanomaterials is the enhanced catalytic activities that some of these materials exhibit. Recently, the peroxidase-like activity of iron oxide nanoparticles has been reported.[32,33] Therefore, we decided to investigate if our DIONrods, being larger and with a different core geometry (nanorods instead of nanospheres), still possess similar peroxidase-like activity. In these experiments, we incubated DIONrods (2 μg of Fe per mL) with the peroxidase-sensitive dye 3,3′,5,5′-Tetramethylbenzidine (TMB, 0.4 mM), which develops a blue color upon oxidation in the presence of hydrogen peroxide and a peroxidase. Results showed that the DIONrods possess peroxidase-like

(32) Gao, L. Z., J.; Nie, L.; Zhang, J.; Zhang, Y.; Gu, N.; Wang, T.; Feng, J.; Yang, D.; Perrett, S.; Yan, X. *Nat. Nanotechnol.* **2007**, *2*, 577z–583.

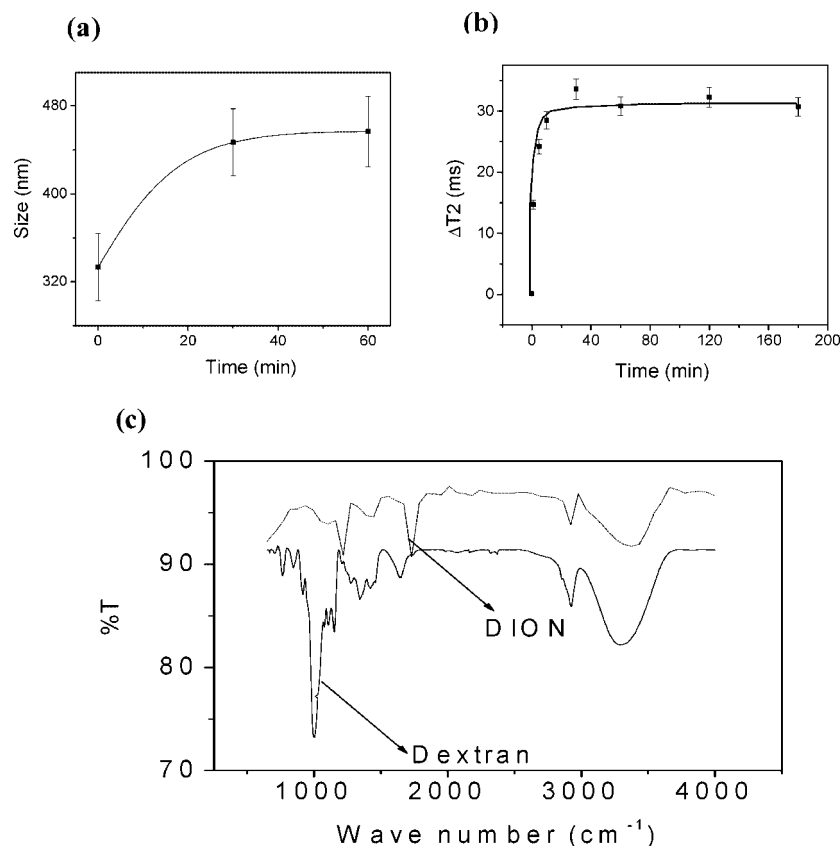(33) Perez, J. M. *Nat. Nanotechnol.* **2007**, *2* (9), 535–536.

(a)

(b)

(c)

Figure 3. (a) Dynamic light scattering study of DIONrods with ConA. (b) Time-dependent response in T2 of DIONrods (200 μL, 0.002 mg of Fe per mL) when treated with 10 μL ConA (1 mg in 1 mL of 1X PBS). (c) FTIR spectra of free dextran and DIONrods.
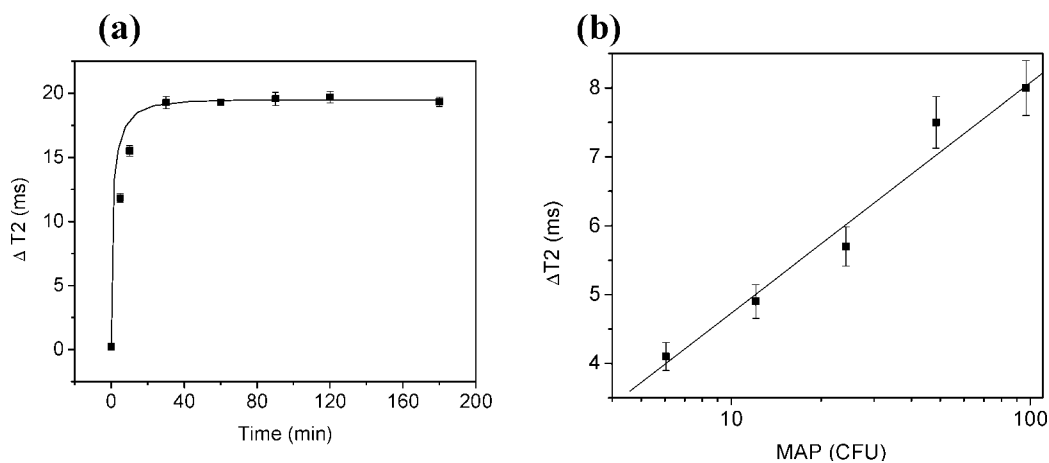
(a)

(b)

Figure 4. (a) Time-dependent response of anti-MAP DIONrods (200 μL, 0.002 mg of Fe per mL) incubated with 100 cfus of MAP in milk after a 30 min incubation. (b) Dose-dependent responses of MAP at different cfus after a 5 min incubation with anti-MAP DIONrods. MAP was diluted in milk and added to the nanosensors' solutions (200 μL, containing 0.002 mg of Fe per mL) and changes in T2 were monitored with respect to control containing milk.

activity as judged by their ability to oxidize the TMB dye in the presence of hydrogen peroxide within 30 min (Figure 5a, vial 2). The observed peroxidase-like activity of our DIONrods is pH-dependent as no oxidation of the dye is observed at pH 7. These results are in line with those recently reported using nanospheres; however, it is worth mentioning that our nanoparticles are bigger, of different shape (nanorods instead of nanospheres), and more magnetic than those previously used. Furthermore, we determined the kinetic parameters of the DIONrods peroxidase-like activity, utilizing TMB as the peroxidase substrate. Specifically, a Michaelis constant, (K_m) of 0.5 mM and a maximal reaction velocity (V_{max}) of 11.6×10^{-8} M/s were obtained from the corresponding LineWeaver−Burk plot (Figure 5b). Notably, the DIONrods' V_{max} is higher than the ones reported for spherical iron oxide nanoparticles and horseradish peroxidase (20 and 33%, respectively), while having TMB as the peroxidase substrate.[32] Furthermore, the DIONrods' affinity toward TMB is 300 times higher than that of iron oxide nanospheres that have a K_m of ∼150 mM.[32] Taken together, these data demonstrate the enhanced intrinsic peroxidase-like activity of our DIONrods.
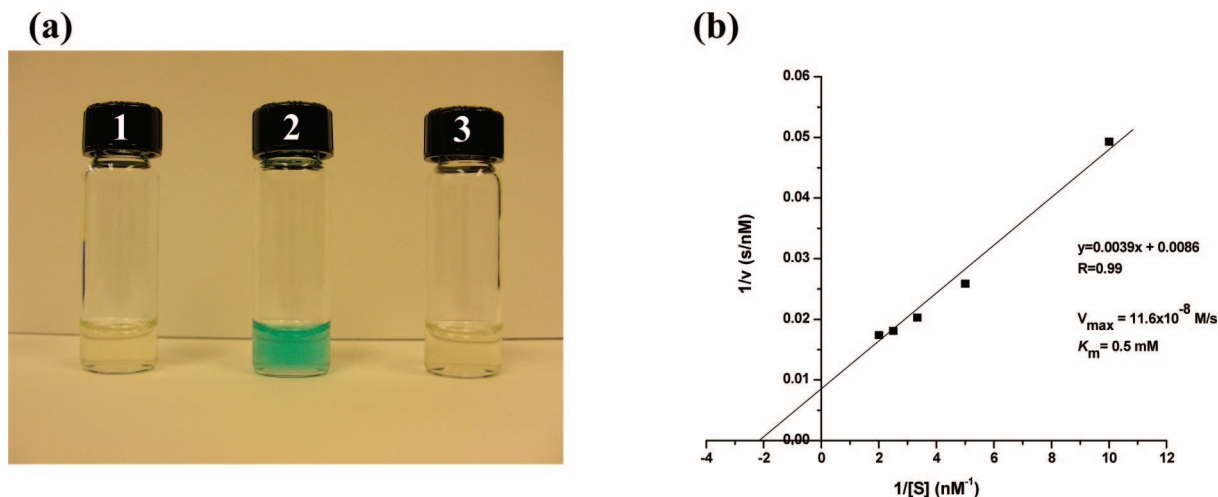
(a)

(b)

Figure 5. (a) Peroxidase-like activity of DIONrods. TMB in citrate buffer (pH 4) was treated with H_2O_2 only as a control (**1**), with H_2O_2 and DIONrods (**2**), and with DIONrods and no H_2O_2 (**3**). (b) Kinetics of peroxidase-like activity of DIONrods prepared from high-purity 10-K dextran (Amersham-GE).

Finally, we investigated the reproducibility and the role of the dextran's purity on the nanorods formation. Previous work by Alivisatos and others has shown that the level of purity of the stabilizer or capping agent plays a key role in the geometry of the resulting nanocrytals.[34] For the synthesis of our DIONrods, we have used a 10-K dextran polymer (Amersham) with a high degree of purity. Therefore, we examined whether dextrans of lower purity could affect the formation of the nanorods. For these studies, we obtained dextrans of different degrees of purity (Sigma, and Fisher) and used them to synthesize dextran-coated iron oxide nanoparticles. We found that high-purity dextrans reproducibly yield monodisperse rods, whereas dextrans of lower purity (Sigma and Fisher) always yield polydisperse spherical nanoparticles using our procedure (see Figure 2 in the Supporting Information). These results are significant as they point to the dextran level of purity as a key factor in the formation of the DIONrods.

It has been reported that dextrans of different molecular weight adopt a particular coil conformation in solutions with distinct dimensions and sizes. For instance, typically a 500-K dextran has a diameter of 29.4 nm (Stokes radius = 14.7 nm), whereas a 10-K dextran is roughly 4.8 nm (Stokes radius $\approx$ 2.4 nm).[35] Hence, through dynamic light scattering (DLS), we determined that the Amersham dextrans had an average diameter of 4.84 nm, with a narrow size distribution (see Figure 2a in the Supporting Information). However, the Sigma and Fisher dextrans had two distinct broad population distributions. Specifically, 87% of the population had an average diameter of 4.8 nm, whereas the remaining 13% had significantly larger size (see Figure 2b in the Supporting Information). Interestingly, this small amount of larger molecular size fractions presumably is enough to affect the shape of the iron oxide nanoparticles (see Figure 2c,d in the Supporting Information). Additionally, the spherical iron oxide nanoparticles obtained with the less pure dextrans displayed poor crystallinity, lower T2 relaxation, and lower

peroxidase activity. Specifically, the peroxidase activity of these spherical nanoparticles is lower than that of the DIONrods (K_m = 1.3 mM; V_{max} = 9.8 $\times$ 10^{-8} M/s) (see Figure 3 in the Supporting Information). The observed formation of iron oxide nanorods, when a high purity dextran polymer with narrow size distribution and average size of 4.84 nm is used, can be explained by the preferential binding of these polymers to particular surfaces in the initially formed iron oxide crystals. This initiates preferential growth of the nanoparticles in one direction. As the number of higher-molecular-weight and therefore larger-sized (>100 nm) dextran impurities increases, they start interfering with this preferential growth process, therefore resulting in a polydisperse spherical iron oxide preparation.

Conclusion

In summary, we have demonstrated a facile, aqueous-based, and room-temperature synthesis of polymer-coated Fe_3O_4 nanorod. The as-synthesized dextran-coated iron oxide nanorods (DIONrods) exhibit superparamagnetic behavior as well as enhanced water spin—spin relaxation and peroxidase activity. Furthermore, their polymer coating can be easily functionalized with amine groups and conjugated with antibodies for targeting and sensing applications. It is expected that this new type of polymer-coated iron oxide nanorod may find use in many applications including magnetic sensing and diagnostics, hyperthermia and imaging, catalytic oxidations, and the fabrication of devices and nanocomposites with dual magnetic and catalytic activity.

Supporting Information Available: (1) Photograph of DIONrods aqueous suspension, (2) DLS and TEM of DIONrods prepared with dextran form different ventors, (3) kinetics of peroxidase activity of DIONrods prepared using a dextran of lower purity (PDF). This material is available free of charge via the Internet at http://pubs.acs.org.

CM8031863

(34) Manna, L. S., E. C.; Alivisatos, A. P. *J. Am. Chem. Soc.* **2000**, *122*, 12700–12706.
(35) Jaiswal, J. K.; Chakrabarti, S.; Andrews, N. W.; Simon, S. M. *PLoS Biol.* **2004**, *2* (8), E233.